Taylor & Francis
Taylor & Francis Group

RESEARCH PAPER

🔓 OPEN ACCESS | Check for updates

Determination of antiviral action of long non-coding RNA loc107051710 during infectious bursal disease virus infection due to enhancement of interferon production

Xuewei Huang[a]*, Yigang Xu [ID][a]*, Qingyu Lin[a]*, Weilong Guo[a], Dongfang Zhao[a], Chunmei Wang[a], Li Wang[a], Han Zhou[a], Yanping Jiang[a], Wen Cui[a], Xinyuan Qiao[a], Yijing Li[a], Guangpeng Ma[b], and Lijie Tang [ID][a]

[a]College of Veterinary Medicine, Northeast Agricultural University, Harbin, P.R. China; [b]Agricultural High Technology Department, China Rural Technology Development Center, Beijing China

ABSTRACT

The functions and profiles of lncRNAs during infectious bursal disease virus (IBDV) infection have not been determined, yet. The objectives of this study were to determine the antiviral action of loc107051710 lncRNA during IBDV infection by investigating the relationship between loc107051710 and IRF8, Type I IFN, STATs, and ISGs. DF-1 cells were either left untreated as non-infected controls (n = 1) or infected with IBDV (n = 3). RNA sequencing was applied for analysis of mRNAs and lncRNAs expression. Differentially expressed genes were verified by RT-qPCR. Then identification, of 230 significantly different expressed genes (182 mRNAs and 48 lncRNA) by pairwise comparison of the infected and control groups, was carried out. The functions of differentially expressed lncRNAs were investigated by selection of lncRNAs and mRNAs significantly enriched in the aforementioned biological processes and signaling pathways for construction of lncRNA-mRNA co-expression networks. The techniques of gene ontology and Kyoto Encyclopedia of Genes and Genomes pathways were applied. It was suggested that these differentially expressed genes were involved in the interaction between the host and IBDV. Loc107051710 was found to have potential antiviral effects. RT-qPCR and western blot were applied and revealed that loc107051710 was required for induction of IRF8, type I IFN, STAT, and ISG expression, and its knockdown promoted IBDV replication. By fluorescence in situ hybridization, it was found that loc107051710 was translocated from the nucleus to the cytoplasm after infection with IBDV. Overall, loc107051710 promoted the production of IFN-α and IFN-β by regulating IRF8, thereby promoting the antiviral activity of ISGs.

Introduction

Infectious bursa disease (IBD) is a highly contagious and immunosuppressive disease that affects young chickens. It causes high mortality rates and large economic losses to the poultry industry [1,2]. Infectious bursal disease virus (IBDV) mainly causes the destruction of B-lymphocytes in the bursa of Fabricius, which can lead to severe immunosuppression and secondary infections in infected chickens [3–5]. The virus (IBDV) is non-enveloped with an icosahedral capsid. It belongs to the family *Birnaviridae*. The genome of IBDV is bi-segmented, double-stranded RNA [6].

While the importance of protein encoding genes has long been known, the various types of noncoding RNAs are increasingly receiving attention [7]. Long noncoding RNAs (lncRNAs), which are composed of more than 200 nucleotides, in particular, are involved in apoptosis during

organ development and tissue differentiation [8]. They also play regulatory roles in many diseases, particularly, human cancers [9–11], and in the adaptive and innate immune responses [8,12]. Moreover, the lncRNAs have antiviral functions by changing the expression levels of IFNs or ISGs against Theiler's virus, encephalomyocarditis virus, hepatitis C virus, influenza A virus, and HIV [13–17].

Although DF-1 cells, a continuous line of chicken embryo fibroblasts, have been used to study the transcriptional changes and differentially expressed proteins of host cells in response to IBDV infections [18–24], the role of host lncRNAs in response to IBDV infection is still unknown. Application, of some sophisticated techniques such as techniques of in depth bioinformatics, RNA sequencing, RT-qPCR, Fluorescence in situ hybridization, and western blotting, is expected to provide a theoretical basis for novel preventive and therapeutic strategies against

IBDV. The objective of this study was to determine the antiviral action of loc107051710 during IBDV infection in cultured DF-1 cells after investigation of the relationship between the loc107051710 and IRF8, type I IFNs, STATs and ISGs. The antiviral action of loc107051710 was determined by application of RNA-seq for analysis of mRNAs and lncRNAs expression. Next, identification of differentially expressed genes by pairwise was carried out. After that, the functions of differentially expressed lncRNAs were investigated by selection of lncRNAs and mRNAs significantly enriched in the aforementioned biological processes and signaling pathways for construction of lncRNA-mRNA co-expression networks. The techniques of GO and KEGG pathways were applied. Subsequently, RT-qPCR and western blot were applied to investigate the relationship between loc107051710 and IRF8, type I IFNs, STATs, and ISGs expression. Eventually, fluorescence in situ hybridization was applied to determine the location of loc107051710.

Materials and methods

Cells and viruses

Chicken embryonic fibroblast DF-1 cells (CRL-12,203, ATCC) were cultured in high-glucose (4.5 g D-glucose/L) Dulbecco's modified Eagle's medium (Life Technologies, Grand Island, NY, USA). Then, this medium was supplemented with 10% fetal bovine serum (Invitrogen, Carlsbad, CA, USA), and the culture was incubated at 37°C with 5% CO_2. IBDV strain CEF94 (College of Veterinary Medicine, Northeast Agricultural University, China) was propagated in DF-1 cells. The tissue culture infectious dose 50 (TCID50) was $10^{5.25}/0.1$ mL. Cells were incubated with IBDV at a multiplicity of infection of 1 (MOI = 1) for 24 h.

Experimental design and RNA extraction for sequencing

The DF-1 cell cultures were divided into two groups. The first group was infected with IBDV (n = 3). The second group was kept without infection as a control (n = 1). The total RNA of the control (n = 1) and IBDV-infected (n = 3) groups was extracted using TRIzol reagent (Invitrogen, Carlsbad, CA, USA) according to the manufacturer's instructions. The purity, concentration, and integrity of the total RNA were analyzed using an Agilent Bioanalyzer 2100 (Agilent Technologies, Santa Clara, CA, USA). Samples with an RNA integrity number (RIN) value > 9.7 and an optical density 260:280 ratio > 2.0 were used for library

construction and deep sequencing. RNA-seq was performed by Novel Bioinformatics Co., Ltd. (Shanghai, China) using the Illumina XTen platform.

Quality control of RNA readings

The raw readings were preprocessed with custom Perl scripts to ensure the high quality of RNA for subsequent analyzes. Adapter-polluted readings, low-quality readings (in which more than 15% of bases had a Phred score ≤ 19, or more than 5% were undetermined, N), and readings matching rRNA were removed.

Alignment, mapping of RNA-seq to reference genome and transcriptome assembly

Using TopHat version 2.0.12 [25] the RNA-seq readings were aligned and mapped to the reference genome obtained from NCBI Gallus_gallus-5.0 (ftp://ftp.ncbi.nlm.nih.gov/genomes). Using the Cufflinks 2.2.1 program [26], the transcriptome of each sample was assembled independently with the help of the reference annotation-based transcript assembly technique.

Selection of lncRNAs

Based on the assembly results, some transcripts were removed such as transcripts with readings of 0. For selection of lncRNAs, the following transcripts were removed: Transcripts which were shorter than 200 nucleotides and having less than two exons, transcripts which were only present in one sample, and transcripts which were encoding a protein family or were a known mRNA transcript. The Coding-Non-Coding Index (CNCI) [27], Coding Potential Calculator (CPC) [28], and Coding-Potential Assessment Tool (CPAT) [29] were used to evaluate the coding potential of the transcripts. Default parameters were used with all the software. After filtering, transcripts without coding potential were considered candidate lncRNAs.

Quantification of gene expression

The read count for each gene in each sample was determined by HTSeq v0.6.0 [30], and the number of fragments per kilobase of transcript sequence per million base pairs sequenced [31] was calculated to measure the expression levels of both mRNAs and lncRNAs in each sample. DESeq v1.16.0 [32] was used for the differential expression analysis of two groups. Genes, with a p value <0.05 and a fold change >1.5, were considered differentially expressed in the two groups.

Determination of significantly enriched biological functions and pathways in mRNAs differentially expressed in IBDV infected DF-1 cells and control DF-1 cells

Using fisher.test and p.adjust routines, 2 analyses were performed with custom R scripts. These 2 analyses were gene ontology (GO) and Kyoto encyclopedia of genes and genomes (KEGG) pathway enrichment. These analyses were used to determine biological functions and pathways significantly enriched in mRNAs differentially expressed in IBDV infected DF-1 cells and control DF-1 cells. GO categories and KEGG pathways with p values <0.05 were considered significantly enriched.

Protein-protein and lncRNA-mRNA co-expression network analyses

We constructed gene co-expression networks to identify the interactions among differentially expressed genes. The gene co-expression networks were built using the normalized signal intensity of specific expression genes. For each pair of genes, the Pearson correlation coefficient was calculated, and significantly correlated pairs were selected to construct the networks. In network analysis, degree centrality* was the simplest and most important measure of the relative importance of a gene within a network. Moreover, to analyze certain properties of the networks, k-cores**, from graph theory, were introduced for simplifying graph topology analysis. In the present study, the purpose of the network structure analysis was to locate genes in one network. When analyzing the different networks, genes with the largest degree of difference between the two classes were selected. (Note: *Degree centrality is defined as the number of links connecting one node to other nodes; **A k-core of a network is a subnetwork in which all nodes are connected to at least k other genes in the subnetwork. Accordingly, a k-core of a protein-protein interaction network contains cohesive groups of proteins).

Gene silencing of loc107051710

A specific siRNA for loc107051710 was designed by Genepharma Co., Ltd. (Shanghai, China). The sequences of the specific and control siRNA are listed in Table 1. In total, 5×10^5 DF-1 cells were seeded in 6-well plates, and when they reached 50–60% confluence, they were transfected with 100 nM negative siCont or siloc107051710 using Lipofectamine 2000 (Invitrogen, Carlsbad, CA, USA) according to the manufacturer's instructions. After transfection for 24 h, the cells were infected for 24 h with IBDV (MOI = 1).

Table 1. SiRNA and probe sequence of loc107051710.

Sequence name	Primer sequence (5′-3′)
Loc107051710-sense	GCAAGACAGCAUUUGGUAUUTT
Loc107051710-antisense	AUACCAAAUGCUGUCUUGCTT
Negative control-sense	UUCUCCGAACGUGUCACGUTT
Negative control-antisense	ACGUGACACGUUCGGAGAATT
Loc107051710-antisense probe	CCAGTATGGAAGAAGTTGAAAATG
Loc107051710-sense probe	TGTTGGTCCTTTGTCTGTGATCAG

Quantitative reverse transcription PCR (Rt-qPCR)

Total RNA was extracted from control and IBDV-infected groups using TRIzol according to procedures previously described and reverse-transcribed to cDNA using M-MLV Reverse Transcriptase (Promega, Madison, WI, USA) according to the manufacturer's procedures. Twenty-four differentially expressed genes were selected to confirm the accuracy of RNA-seq by RT-qPCR, including 12 lncRNAs and 12 mRNAs. Moreover, RT-qPCR was applied for detection of the expression of type I IFNs, STATs and ISGs. Primers were designed using oligo6 software (Tables 2–4). For RT-qPCR, the ABI 7500 Real-Time PCR system (Applied Biosystems, Carlsbad, CA, USA) and SYBR Green Master (TaKaRa, Dalian, China) were used; the reactions were performed in a final volume of 20 μL. The *GAPDH* gene was used as an internal control. The relative fold change was calculated by the $2^{-\Delta\Delta Ct}$ method [33]. Experiments were repeated three times.

Western blotting

Total proteins were extracted, subjected to 15% SDS-PAGE and transferred to PVDF membranes. After blocking with

Table 2. RT-qPCR primers used for verification of mRNA results.

Gene	Primer sequence (5′-3′)	Accession number
GAPDH	F-TGACCACTGTCCATGCCATC R-CAGCAGCCTTCACTACCCTC	NM_204305
IFI6	F-TCAGGCTTTACCAGCAGTGG R-TGCCACCCATTGAGATAGACTG	NM_001001296
IRF1	F-TAAGCATGGCTGGGACATGG R-GGAGCATCCTGTACACTCGG	XM_015294015
IFIT5	F-CCCTCTCAAGCTGAAGCACT R-TGAACAGACAAGCAAACGCA	NM_001320422
TLR3	F-ACATTTGTAACACCCCGCCT R-CCCGGTAGTCTGTCAAGCTC	FJ915471
RSAD2	F-GCAGTGCAACTACAAGTGTG R-GAAATGGTTCTCCTCCTGAG	NM_001318443
OASL	F-GTCAGCATCACCAGTCCG R-CAGTGCGTCGTAAGCAGG	XM_015293006
DUSP18	F-GTGCAAGGAGGAAGGAGGA R-GACGGTGGTGATGTGGTTG	XM_415295.6
BEST3	F-GGAACGATTCTTCTGCACG R-GGAAGAACACCGAGTTCTCAC	NM_001199669.1
ZNF414	F-GAAGCACTACGCCTGCTCCAG R-AAGGTCTCTGTGCAGCCCAGC	XM_015299849.2
PLVAP	F-AACCTGACACGAACCCTCAAC R-CCTTCTGATGTCCTCTAGCCTG	XM_003643487.4
CCLi10	F-CTCTGCTCCTCGGCTGTG R-AGGCAATGAGGTTGCGTG	FR874034.1
TNS4	F-TGTCCCACCCAGCCTCTC R-GGAGGGGTACCCCACCTG	XM_015299654.2

Table 3. RT-qPCR primers used for verification of lncRNA results.

Gene	Primer sequence (5′-3′)	Accession number
loc107051710	F-GAGGAATTGAGGAGTGAGTG R-ATGTCCTGGTCCTCGTTC	XR_001463517
loc107052218	F-GAGTCCCAGGACAGCATG R-AAGTCTGGCTGGTGGCTG	XR_001464528
loc107052259	F-CAATCACAGAGCAGTGCG R-CTGCATTCCAGGGTGAGG	XR_001464642.2
loc107050176	F-GGGAGCTGCGAAGGATGAGT R-CCAGCGCTCCAAAGCTTCAC	XR_001462440
loc107053553	F-CAGCAGTGCTCCCAGCAG R-ACCTGGTGAGGGCAGGCT	XR_001466914
loc107052689	F-ACCTCCTCCTTGTGGAAG R-ACCTGCAGTTTCACAGGG	XR_001465330
loc107053273	F-TGTTGGGTGTACGTCCTTC R-ATCGGTGGTATCTGACAGC	XR_003074877.1
loc107054529	F-CCATGCAAGCTGTGTGAG R-CAGTCCATCTGCATGCAC	XR_001468879.1
loc107052150	F-CGAACTCCAGAGGAACTG R-TCAAGCCCATAGATGCAG	XR_001464380.2
loc107054795	F-GGCCTATTCTATGCAGCATG R-CAGAAGAAGGGCTCATGAAG	XR_003071209.1
loc107052781	F-AGGCGAATAGCAGAGGTAC R-GCTCAGAGCTCCAGTAAAG	XR_001465506.2
loc107055337	F-CAAGATCACCAGGTGCAAC R-CCTGTTGGGTCATGACATG	XR_001470403.2

Table 4. RT-qPCR primers sequences.

Gene	Primer sequence (5′-3′)	Accession number
OAS	F-CCACATCCTCGCCATCATCG R-GTCTGTCCCGGCTGTCCTTG	NM_205041
Mx1	F-GGTGTCATTACTCGCTGT R-CTTTCTTCACCTCTGATGC	GU256272
PKR	F-GGCACCAGAACAGTTTGG R-GTTCAGTGGAAGGTCACC	AB125660
STAT1	F-CGATGACAGCTTTCCTATGG R-GCAGGTCATGGAATAGCAC	XM_015289392
STAT2	F-CCCGAGAACTTTGCCAACC R-GATCTCCTGCTCCTGGCTG	XM_015300285
IRF8	F-CCGTCAGAAGCAGATCACCA R-TTGCTTGGCCTGTCCTTGTA	XM_015292553
IFN-α	GACATGGCTCCCACACTACC AGGCGCTGTAATCGTTGTCT	GU119896
IFN-β	CCTCAACCAGATCCAGCATT GGATGAGGCTGTGAGAGGAG	GU119897
IBDV-VP2	F- GTCAAGCACACTTCCTGGTG R- GTCGTTGATGTTGGCTGTTG	AF194428

5% skim milk overnight, the PVDF membranes were incubated at 37°C for 1 h with anti-chicken IFN-α and IFN-β antibodies (1:1000; Cloud-Clone Corp, Houston, TX, USA) and anti-IBDV VP2 polyclonal antibodies (1:500) prepared in our laboratory. Subsequently, the samples were incubated with horseradish peroxidase-conjugated goat anti-rabbit IgG secondary antibodies (1:3000; Cloud-Clone Corp., Houston, TX, USA) at 37°C for 40 min, and the immunoblots were visualized with an enhanced chemiluminescence system (Cheml Scope5300; Clinx Science Instruments, Shanghai, China). β-actin was used as an internal control.

Fluorescence in situ hybridization (FISH)

Using FISH technique, loc107051710 was detected on DF-1 cells. The biotin-labeled antisense and sense probes of loc107051710 were synthesized by RiboBio (Guangzhou, China) and the sequences are listed in Table 1. The FISH assay was performed using a Fluorescent In Situ Hybridization Kit (RiboBio, Guangzhou, China) according to the manufacturer's procedures. In brief, DF-1 cells were fixed with 4% polyoxymethylene. After washing with PBS, the cells were treated with 0.5% Triton X-100 at 4°C for 5 min. Next, the cells were treated with pre-hybridization lncRNA FISH probe mix at 37°C for 30 min. Hybridization was performed by the adding antisense and sense loc107051710 FISH probe mix (10 mM ATP, 10 mM CTP, 10 mM GTP, 6.5 mM UTP and 3.5 mM Biotin-16-UTP), followed by incubation at 37°C overnight. After washing with 4×, 2×, and 1× SSC, the cells were stained with DAPI, washed three times with PBS, and visualized by laser scanning confocal microscopy.

Statistical analyses

The data were analyzed using GraphPad Prism5 software. One-way ANOVA was used to determine significance. P values <0.05 were considered statistically significant.

Results

Overview of lncRNA and mRNA expression profiles

In total, 361 100 380 raw reads were obtained from the infected and control DF-1 cells (NCBI SRA Run Selector, accession number SRP145165). After quality control, 308 057 830 clean reads (readings after removal of Adapter-polluted readings, low-quality readings and readings matching rRNA), were obtained, and the percentage of clean reads ranged from 83.74% to 87.27%. The percentage of clean reads with a Phred quality value of more than 30 ranged from 95.03% to 95.54% (Table 5). Overall, 86-87% of the clean reads aligned with the chicken reference genome (Table 6).

Identification of differentially expressed lncRNAs and mRNAs

To analyze the differential expression of mRNAs and lncRNAs between the control and IBDV-infected groups, heat maps (Figure 1(a)) and volcano plots (Figure 1(b)) were generated. Given the criteria of p value <0.05 and fold change >1.5, 91 mRNAs were upregulated and 91 were downregulated (Table 7, supplementary materials 1) . Furthermore, 13 lncRNAs were upregulated, and 35 lncRNAs were downregulated in IBDV- infected DF-1 cells (Table 7, supplementary materials 2).

Table 5. Data quality of lncRNA and mRNA profiles.

Sample name	Raw reads	Clean reads	Clean reads rate (%)	Q30 (%)
JD01c	81,795,032	68,492,856	83.74	95.03
JD02c	83,442,316	69,873,950	83.74	95.07
JD03c	93,319,420	81,440,754	87.27	95.54
CK01c	102,543,612	88,250,270	86.06	95.22

Table 6. Clean reads compared with the reference genome.

	Samples			
	CK01C	JD03C	JD01C	JD02C
Total Reads	88,129,420	81,326,852	68,412,444	69,781,248
Mapped Reads	76,989,566	70,851,841	58,920,072	60,073,583
Mapping Rate (%)	0.87	0.87	0.86	0.86
UnMapped Reads	11,139,854	10,475,011	9,492,372	9,707,665
MultiMap Reads	2,064,678	1,904,761	1,616,128	1,643,890
MultiMap Rate (%)	0.02	0.02	0.02	0.02

Functional annotation of differentially expressed mRNAs

In total, 182 differentially expressed mRNAs were subjected to GO and KEGG pathway enrichment analyses (Figures 2 and 3) to obtain a better understanding of the potential roles of host factors in IBDV infection. We found that the GO terms were significantly enriched in differentially expressed mRNAs, as well as for just upregulated mRNAs, were mainly involved in biological processes and pathways that may be related to the replication of IBDV, including the type I IFN signaling pathway, defense response to virus, IFN-γ-mediated signaling pathway, and positive regulation of the type I IFN production signaling pathway (Figure 2 and supplementary materials 3). Moreover, KEGG analysis showed that differentially expressed genes were involved in the RIG-I-like receptor, NF-κB, Toll-like receptor, influenza A, and hepatitis C signaling pathways (Figure 3, supplementary materials 4).

Protein-protein interaction network analysis

mRNA-mRNA functional interaction network analysis demonstrated that *IFIT5, OASL, USP18, TLR3, IRF1, IFI6, SAMD9L, EPSTI1*, and several other mRNAs were at the core of the network (Figure 4). Most of these mRNAs were upregulated and significantly enriched in the type I IFN signaling pathway and the RIG-I, NF-κB, and Toll-like receptor signaling pathways.

lncRNA-mRNA co-expression network analysis

To further examine the functions of the differentially expressed lncRNAs, lncRNA-mRNA co-expression networks were constructed. We first identified and selected the differentially expressed mRNAs and lncRNAs significantly enriched in GO terms and pathways related to the replication of IBDV. We then constructed and analyzed 10 lncRNA-mRNA co-expression networks (Figure 5). The lncRNA-mRNA gene pair loc107051710-*IRF8* had the best correlation.
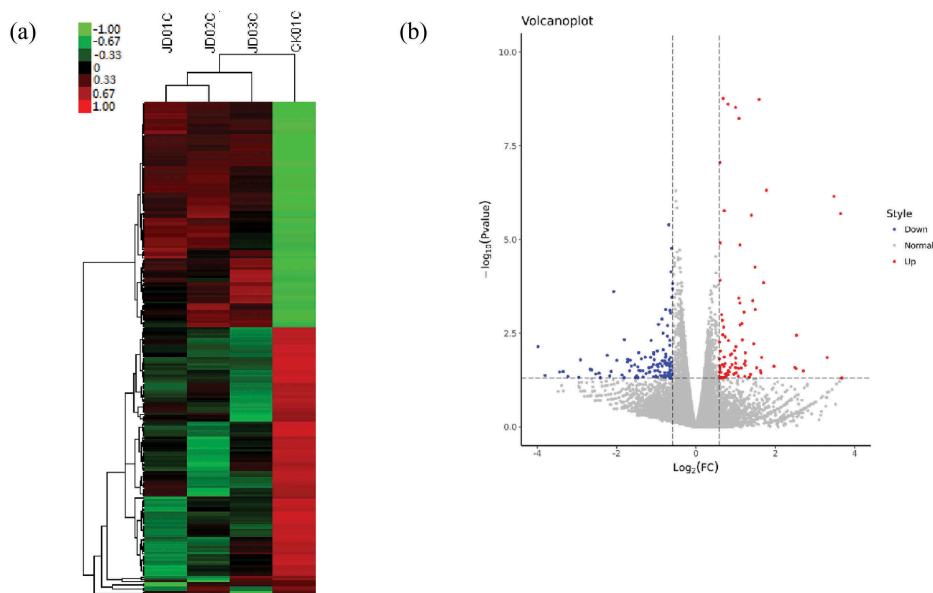

Figure 1. RNA-seq analyses analysis of IBDV-infected DF-1 cells. (a) Heatmap of differentially expressed mRNAs and lncRNAs. Red represents a higher transcription, and green represents a lower transcription. (b) Volcano plots of differentially expressed mRNAs and lncRNAs. The red, blue, and gray dots represent significantly upregulated genes, significantly downregulated genes, and unchanged genes, respectively.

Table 7. The number of differentially expressed mRNA and lncRNA in IBDV treated group.

Comparison	Up-regulated	Down-regulated
mRNA	91	91
LncRNA	13	35

Validation of RNA-seq data by Rt-qPCR

To confirm the accuracy of RNA-seq, several differentially expressed mRNAs and lncRNAs were selected and analyzed by RT-qPCR. The RT-qPCR results were consistent with those from RNA-seq (Figure 6(a,b)), indicating the validity of the RNA-seq data.

Effect of silencing lncRNA loc107051710 on IBDV replication

To further illustrate the association of the loc107051710 with *IRF8*, the lncRNA was knocked-down in DF-1 cells using a specific siRNA. The siRNA for loc107051710 was effective in reducing the expression of the lncRNA (Figure 7(a)). Moreover, the decrease in loc107051710 expression was accompanied by a decrease in *IRF8* expression (Figure 7(b)). To determine whether the reduction in loc107051710 expression resulted in the reduction of type I IFNs (IFN-α and IFN-β), STATs (STAT1 and STAT2), and ISGs (OAS, Mx1, and PKR) expression, their expression levels were measured by RT-qPCR. Surprisingly, silencing loc107051710 decreased the levels of type I IFNs, STATs, and ISGs (Figures 8 and 9). To verify the antiviral effect of loc107051710, we infected siControl or siloc107051710-transduced DF-1 cells and measured the expression of IBDV. The results revealed that IBDV replication was increased by loc107051710 knockdown (Figure 10).
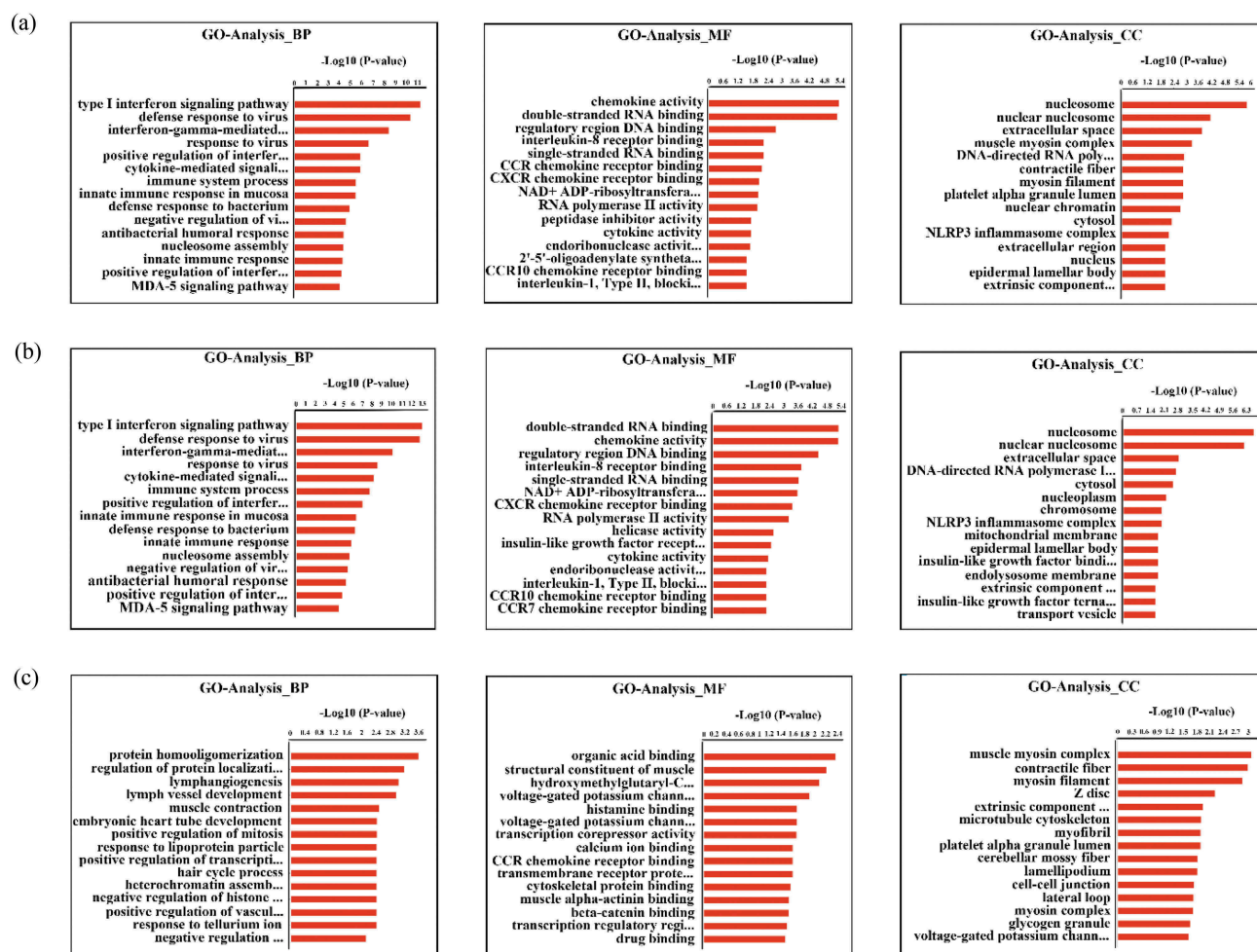

Figure 2. GO enrichment of mRNAs differentially expressed in the infected and control groups with a fold change >1.5 and a *p* value <0.05. (a) Biological process enrichment analysis of all differentially expressed mRNAs. (b) Biological process enrichment analysis of upregulated mRNAs. (c) Biological process enrichment analysis of downregulated mRNAs. The Y-axis shows the pathways, and the X-axis shows the negative logarithm of the *p* value (-log *P*).
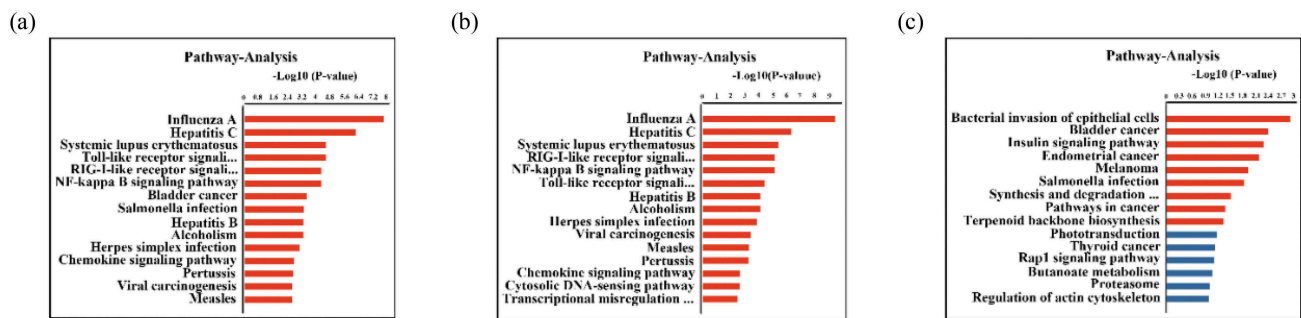
(a)

(b)

(c)

Figure 3. KEGG pathway enrichment of differentially expressed mRNAs with a fold change >1.5 and a p value <0.05. (a) Pathway enrichment analysis of all differentially expressed mRNAs. (b) Pathway enrichment analysis of upregulated mRNAs. (c) Pathway enrichment analysis of downregulated mRNAs. The Y-axis shows the pathways, and the X-axis shows the negative logarithm of the p value (-log P).
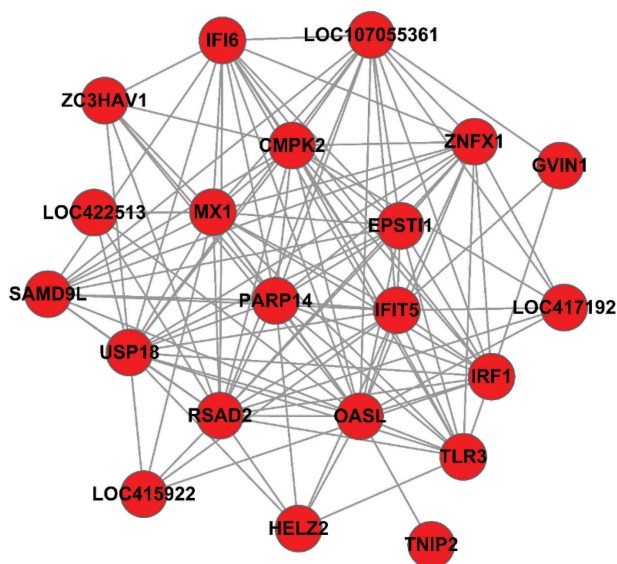
Figure 4. Protein-protein interaction network. A node indicates a differentially expressed mRNA. A node linked to more nodes indicates that it is more important relative to other nodes in this network.

Determination of location of loc107051710 in DF-1 cells by application of fluorescence in situ hybridization

Using FISH, loc107051710 was detected in both the cytoplasm and nucleus of uninfected DF-1 cells (Figure 11(a–c)). However, it was mainly detected in the cytoplasm after infection with IBDV (Figure 11 d-f), and the results showed that Loc107051710 did not bind to the sense probe in IBDV-infected DF-1 cells (g-i).

Discussion

IRFs are a family of transcription factors that were originally isolated as positive and negative regulators of IFNs and IFN-responsive genes [34]. More recently, extensive studies of the IRF family have confirmed that IRFs have gained great attention due to their diverse roles such as in the initiation of antiviral responses, regulation of inflammatory cytokine expression, and control of cell cycle and apoptosis [35,36]. Numerous pattern recognition receptor that can detect cytosolic nucleic acids have been identified and most of them can evoke type I IFN responses via activation of IRFs [37]. The biological activities of type I IFN are initiated by binding to the type I IFN receptor. This leads to the activation of the receptor associated tyrosine kinases JAK1 and Tyk2, which phosphorylate STAT1 and STAT2. Phosphorylated STAT1 and STAT2 interact strongly with DNA-binding protein IRF-9. The IRF-9-STAT1-STAT2 heterotrimer is called ISGF3, which participates in the induction of the expression of ISGs, including OAS, Mx1 and PKP [38]. These ISGs can directly inhibit the replication, assembly and proliferation of the virus. To date, eight IRF homologues have been identified in chickens, though their functions are not yet well defined [39]. *IRF8* (also known as IFN consensus sequence-binding protein [ICSBP]), a member of the IRF family, is expressed by B cells, dendritic cells (DCs) and macrophages, and has a role in the regulation of innate immune responses [40,41]. As an important transcription mediator, *IRF8* is also required for type I IFN induction in virus-stimulated DCs [42]. It appears that *IRF8* is involved in the transcriptional regulation of type I IFN genes; *IRF8* can bind to promoters of IFN-α/β genes to promote the transcription of IFN-α/β [43]. Accordingly, it plays a critical role in the initiation of host innate immune responses to viral infection.

It is well known that host cells can regulate the expression levels of various mRNAs during viral infection. In the current study, differentially expressed
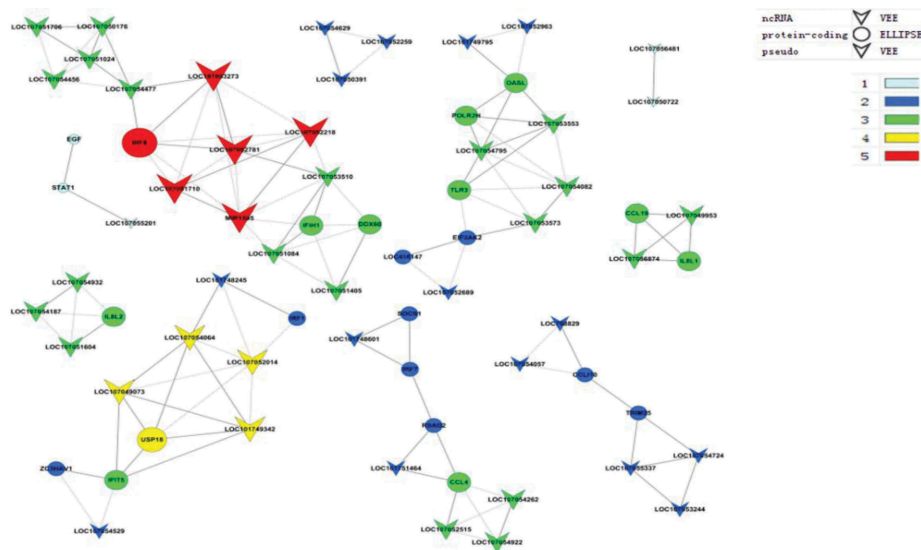
Figure 5. LncRNA-mRNA co-expression networks. A dot represents a differentially expressed mRNA, and a triangle represents a differentially expressed lncRNA. Genes in the same k-core are indicated with the same color. The progression from gray to red represents increasing k for the k-core. The color scale bar is shown.
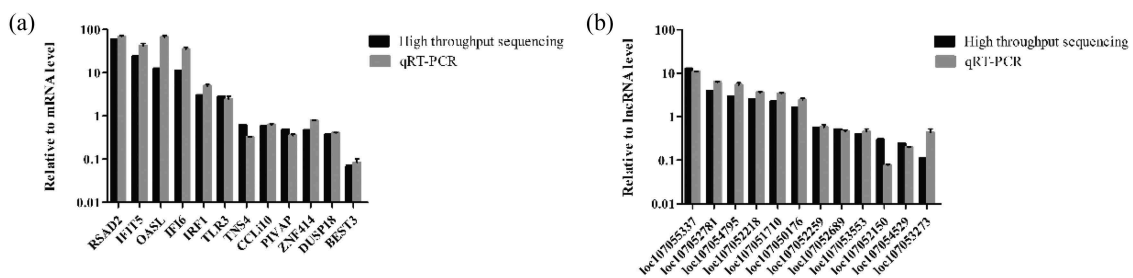

Figure 6. Validation of differentially expressed mRNAs and lncRNAs by RT-qPCR. (a) Transcript levels of mRNAs. (b) Transcript levels of lncRNAs. RT-qPCR experiments were performed in triplicate.
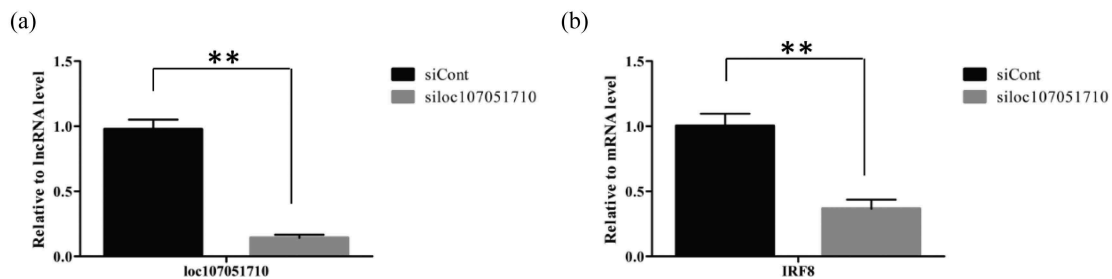

Figure 7. Effect of silencing loc107051710 on *IRF8* expression. DF-1 cells were transfected with either the siControl or siloc107051710 and then infected with IBDV (MOI = 1) for 24 h. The expression levels of loc107051710 and *IRF8* were analyzed by RT-qPCR. RT-qPCR experiments were performed in triplicate. Significant differences between the treated and control groups are indicated as **$P < 0.01$.

mRNAs were analyzed by RNA-seq in DF-1 cells after infection with IBDV. Many of these mRNAs were associated with the antiviral responses of DF-1 cells. Previous studies have demonstrated that IBDV infections induce the expression of different cytokine genes [18]. Furthermore, the genes of cytokines that initiate inflammatory responses, including the *IL8*, nitric oxide synthase, and cyclooxygenase-2 genes, were reported to be upregulated [44,45]. In the present study, we similarly found that the expression of *STAT1, IL8L1,* and *IL8L2* was increased in DF-1 cells after infection with IBDV. Regulatory factors that could modulate the expression levels of these cytokine genes were also over-expressed, including IFN-induced GTP-binding
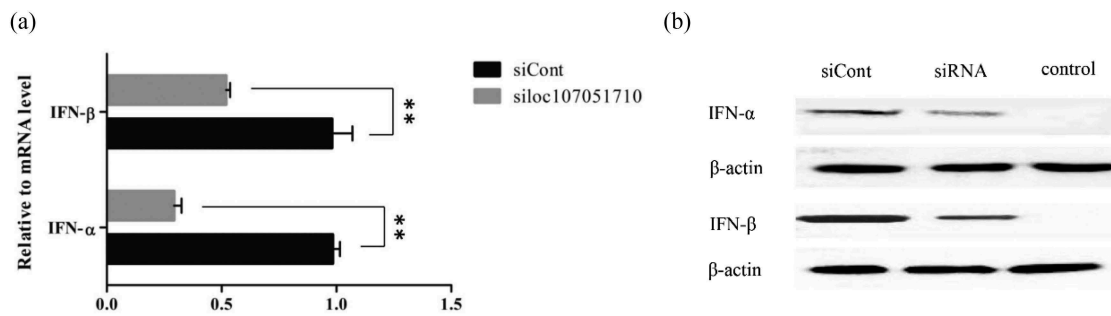
(a)

(b)

Figure 8. Effect of loc107051710 silencing on IFN-α and IFN-β production. DF-1 cells were transfected with either the siControl or siloc107051710 and then infected with IBDV (MOI = 1) for 24 h. The expression levels of IFN-α and IFN-β were measured by RT-qPCR and western blotting. (a) Changes in IFN-α and IFN-β mRNA levels. (b) Changes in IFN-α and IFN-β protein levels. RT-qPCR experiments were performed in triplicate. Significant differences between the treated and control groups are indicated as **$P < 0.01$.
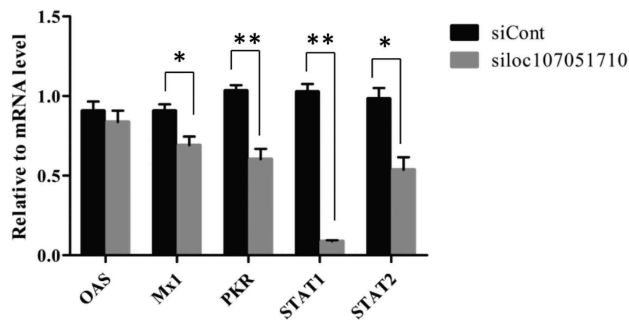

Figure 9. Effect of loc107051710 silencing on ISGs and STATs transcription. DF-1 cells were transfected with either the siControl or siloc107051710 and then infected with IBDV (MOI = 1) for 24 h. The expression levels of ISGs and STATs were measured by RT-qPCR. The experiments were performed at least in triplicate. Significant differences between the treated and control groups are indicated as *$P < 0.05$ and **$P < 0.01$, respectively.

protein Mx1 and IFN-induced protein with tetratricopeptide (IFIT). *IFIT5* is a member of the IFIT family, which can be triggered by viral infection [46] and enhances the antiviral response by promoting IRF3- and NF-κB-mediated gene expression [47]. Our results showed that *IFIT5* expression was 23.8-fold higher and that expression of the NF-κB-mediated genes *IL8L1* and *IL8L2* were 1.58-fold and 1.52-fold higher, respectively, in the infected group than in the control groups.

Radical S-adenosyl methionine (RSAD2) is an endoplasmic reticulum-associated virus inhibitory protein that can be induced by double-stranded RNA viral infection [48], as well as in an IFN-independent pathway by *IRF1* [49]. In our study, *IRF1* and *RSAD2* expression were 3.01-fold and 58.4-fold higher, respectively. Although the specific antiviral mechanism of *RSAD2* has not yet been determined, it is thought to indirectly inhibit viral replication by regulating cell survival [50]. Moreover, the upregulation of the tripartite motif-containing 25 (TRIM25) protein at the beginning of the infection may be associated with RIG-I in the detection of viral RNA intermediates [51]. A previous study has demonstrated that RIG-I can upregulate type I IFNs and reduce viral gene expression [52]. Our results showed that *TRIM25* expression was increased 1.6-fold, and the RIG-I-like receptor signaling pathway was significantly enriched during infection. The differential expression patterns of these
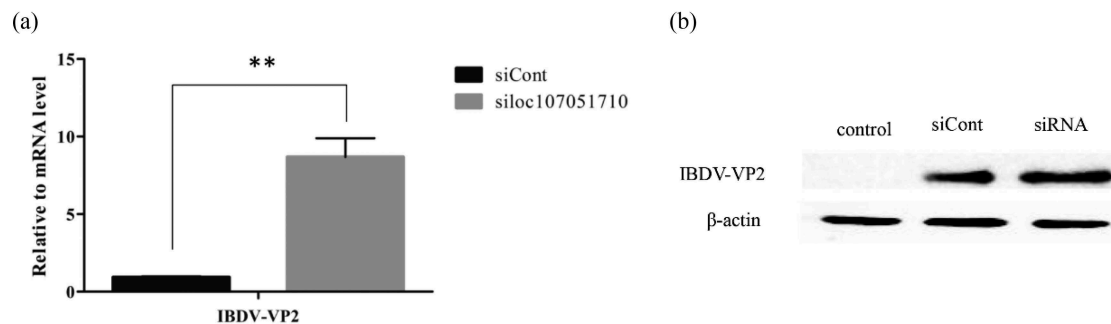
(a)

(b)

Figure 10. Effect of silencing loc107051710 silencing on IBDV VP2 production. DF-1 cells were transfected with siControl or siloc107051710 and then infected with IBDV (MOI = 1) for 24 h. The level of IBDV VP2 expression was measured by RT-qPCR and western blotting. (a) Changes in IBDV VP2 mRNA levels. (b) Changes in IBDV VP2 protein levels. RT-qPCR experiments were performed in triplicate. Significant differences between the treated and control groups are indicated by **$P < 0.01$.
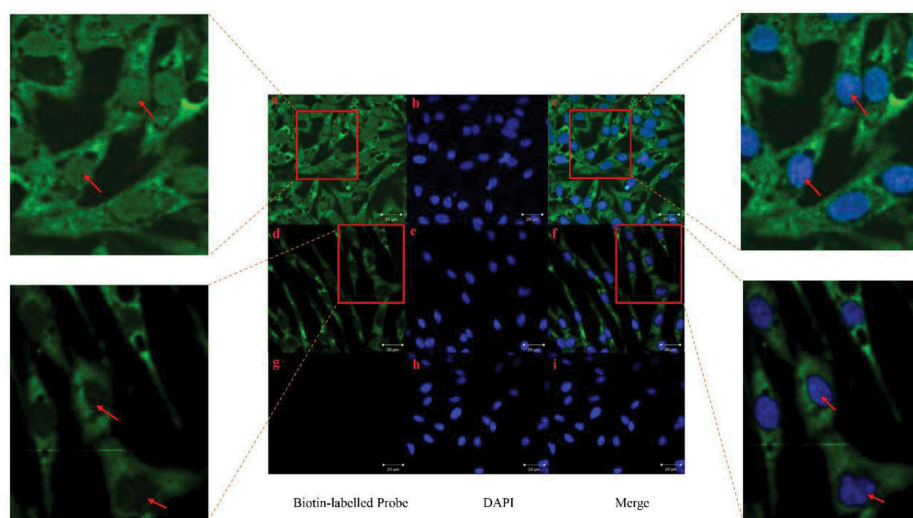
Figure 11. RNA FISH analysis of loc107051710 localization in IBDV-infected DF-1 cells 12 h post infection. (a–c) Non-infected DF-1 cells with antisense loc107051710 probe; (d–f) IBDV-infected DF-1 cells with antisense loc107051710 probe; (g–i) IBDV-infected DF-1 cells with sense loc107051710 probe. The nucleus is stained blue with DAPI. Green indicates the location of the loc107051710 probes.

mRNAs were consistent with those reported in previous studies. We believe that these over-expressed mRNAs may enhance the antiviral ability of DF-1 cells during the early stage of IBDV infection.

In this study, the type I IFN signaling pathway showed the highest enrichment. Type I IFNs can up-regulate the expression of hundreds of ISGs by activating the well-characterized JAK-STAT pathway [53]. Several studies have shown that ISGs induced by type I IFNs contribute to the antiviral response [54,55]. To determine whether differentially expressed lncRNAs play an antiviral role in IBDV-infected DF-1 cells by regulating interferon expression, we first screened out differentially expressed mRNAs significantly enriched in the GO terms and KEGG signaling pathways with antiviral activity. Next, we selected all the differentially expressed lncRNAs and mRNAs enriched in the GO terms and KEGG pathways to construct 10 lncRNA-mRNA co-expression networks. While there were many regulatory relationships in the networks, loc107051710, loc107052218, loc107052243, and loc107052781 had a close relationship with the *IRF8* gene, of which loc107051710 and *IRF8* gene pair had the closest relationship.

We confirmed the cascade relationship between loc107051710 and *IRF8* and found that loc107051710 positively regulates the expression of *IRF8*. In addition, we found that loc107051710 acts as a positive transcriptional regulator of the antiviral-related IFN-α, IFN-β, STAT1, STAT2, OAS, Mx1 and PKR. Therefore, we speculate that loc107051710 promotes the production of IFN-α and IFN-β by regulating *IRF8*, thereby promoting ISGs antiviral activity. However, whether loc107051710 directly regulates *IRF8* expression remains unknown.

The loc107051710 seems to possess antiviral function. However, it was unclear where loc107051710 was localized in uninfected cells and where it exerted antiviral effects after DF-1 cells were infected with IBDV. FISH showed that the amount of loc107051710 increased and shifted from the nucleus to cytoplasm during infection, indicating that it plays an antiviral role not only at the transcriptional level, but also at the post-transcriptional level. Therefore, the antiviral potential of the loc107051710 may be greater than the other lncRNAs analyzed in this study.

In conclusion, we profiled lncRNAs and mRNAs from IBDV-infected DF-1 cells, and based on GO and KEGG pathway enrichment analyses, we identified the differentially expressed mRNAs with antiviral functions. Notably, lncRNA-mRNA co-expression analysis revealed the potential antiviral function of the loc107051710, which involved the regulation of type I IFN, STAT, and ISG production to prevent IBDV infection. In brief, it was concluded that down-regulation of the long non-coding RNA loc107051710 enhanced the replication of infectious bursal disease virus by reducing interferon production. Vice versa up-regulation of the long non-coding RNA loc107051710 suppressed the replication of infectious bursal disease virus by elevated interferon production. Our findings provide a valuable foundation for future studies of the molecular mechanisms of innate anti-IBDV responses in DF-1 cells.

ORCID

Yigang Xu http://orcid.org/0000-0001-7085-7227
Lijie Tang http://orcid.org/0000-0002-2423-0076

References

[1] Li Z, Wang Y, Li X, et al. Critical roles of glucocorticoid-induced leucine zipper in infectious bursal disease virus (IBDV)-induced suppression of type I Interferon expression and enhancement of IBDV growth in host cells via interaction with VP4. J Virol. 2013;87:1221–1231.

[2] Vukea PR, Willows-Munro S, Horner RF, et al. Phylogenetic analysis of the polyprotein coding region of an infectious South African bursal disease virus (IBDV) strain. Infect Genet Evol. 2014;21:279–286.

[3] Faragher JT, Allan WH, Cullen GA. Immunosuppressive effect of the infectious bursal agent in the chicken. Nat New Biol. 1972;237:118–119.

[4] Hudson L, Pattison M, Thantrey N. Specific B lymphocyte suppression by infectious bursal agent (Gumboro disease virus) in chickens. Eur J Immunol. 1975;5:675–679.

[5] Muller H, Islam MR, Raue R. Research on infectious bursal disease–the past, the present and the future. Vet Microbiol. 2003;97:153–165.

[6] Tacken MG, Thomas AA, Peeters BP, et al. VP1, the RNA-dependent RNA polymerase and genome-linked protein of infectious bursal disease virus, interacts with the carboxy-terminal domain of translational eukaryotic initiation factor 4AII. Arch Virol. 2004;149:2245–2260.

[7] Kowalczyk MS, Higgs DR. Molecular biology RNA discrimination. Nature. 2012;482:310.

[8] Wang P, Xue Y, Han Y, et al. The STAT3-binding long noncoding RNA lnc-DC controls human dendritic cell differentiation. Science. 2014;344:310–313.

[9] Liu H, Li J, Koirala P, et al. Long non-coding RNAs as prognostic markers in human breast cancer. Oncotarget. 2016;7:20584–20596.

[10] Ricciuti B, Mencaroni C, Paglialunga L, et al. Long noncoding RNAs: new insights into non-small cell lung cancer biology, diagnosis and therapy. Med Oncol. 2016;33:18.

[11] Jiang X, Liu W. Long noncoding RNA highly upregulated in liver cancer activates p53-p21 Pathway and promotes nasopharyngeal carcinoma cell growth. DNA Cell Biol. 2017;36:596–602.

[12] Li Z, Chao TC, Chang KY, et al. The long noncoding RNA THRIL regulates TNFalpha expression through its interaction with hnRNPL. Proc Natl Acad Sci U S A. 2014;111:1002–1007.

[13] JA G, OL W, YW Y, et al. The NeST long ncRNA controls microbial susceptibility and epigenetic activation of the interferon-gamma locus. Cell. 2013;152:743–754.

[14] Nishitsuji H, Ujino S, Yoshio S, et al. Long noncoding RNA #32 contributes to antiviral responses by controlling interferon-stimulated gene expression. Proc Natl Acad Sci U S A. 2016;113:10388–10393.

[15] Xiong Y, Yuan J, Zhang C, et al. The STAT3-regulated long non-coding RNA Lethe promote the HCV replication. Biomed Pharmacother. 2015;72:165–171.

[16] Ouyang J, Zhu X, Chen Y, et al. NRAV, a long non-coding RNA, modulates antiviral responses through suppression of interferon-stimulated gene transcription. Cell Host Microbe. 2014;16:616–626.

[17] Carnero E, Barriocanal M, Segura V, et al. Type I Interferon Regulates the Expression of Long Non-Coding RNAs. Front Immunol. 2014;5:548.

[18] Li YP, Handberg KJ, Juul-Madsen HR, et al. Transcriptional profiles of chicken embryo cell cultures following infection with infectious bursal disease virus. Arch Virol. 2007;152:463–478.

[19] Wong RT, Hon CC, Zeng F, et al. Screening of differentially expressed transcripts in infectious bursal disease virus-induced apoptotic chicken embryonic fibroblasts by using cDNA microarrays. J Gen Virol. 2007;88:1785–1796.

[20] Hui RK, Leung FC. Differential expression profile of chicken embryo fibroblast DF-1 cells infected with cell-adapted infectious bursal disease virus. PLoS One. 2015;10:e0111771.

[21] Lin J, Xia J, Zhang K, et al. Genome-wide profiling of chicken dendritic cell response to infectious bursal disease. BMC Genomics. 2016;17:878.

[22] Zheng X, Hong L, Shi L, et al. Proteomics analysis of host cells infected with infectious bursal disease virus. Mol Cell Proteomics. 2008;7:612–625.

[23] Wu Y, Peng C, Xu L, et al. Proteome dynamics in primary target organ of infectious bursal disease virus. Proteomics. 2012;12:1844–1859.

[24] Foster DN. Development of a spontaneously immortalized chicken embryo fibroblastic cell line. 1998.

[25] Langmead B, Trapnell C, Pop M, et al. Ultrafast and memory-efficient alignment of short DNA sequences to the human genome. Genome Biol. 2009;10:R25.

[26] Roberts A, Pimentel H, Trapnell C, et al. Identification of novel transcripts in annotated genomes using RNA-Seq. Bioinformatics. 2011;27:2325–2329.

[27] Sun L, Luo H, Bu D, et al. Utilizing sequence intrinsic composition to classify protein-coding and long non-coding transcripts. Nucleic Acids Res. 2013;41:e166.

[28] Kong L, Zhang Y, Ye ZQ, et al. CPC: assess the protein-coding potential of transcripts using sequence features and support vector machine. Nucleic Acids Res. 2007;35:W345–349.

[29] Wang L, Park HJ, Dasari S, et al. CPAT: coding-potential assessment tool using an alignment-free logistic regression model. Nucleic Acids Res. 2013;41:e74.

[30] Anders S, Pyl PT, Huber W. HTSeq–a Python framework to work with high-throughput sequencing data. Bioinformatics. 2015;31:166–169.

[31] Trapnell C, Williams BA, Pertea G, et al. Transcript assembly and quantification by RNA-Seq reveals unannotated transcripts and isoform switching during cell differentiation. Nat Biotechnol. 2010;28:511–515.

[32] Anders S, Huber W. Differential expression analysis for sequence count data. Genome Biol. 2010;11:R106.

[33] Cyplik P, Schmidt M, Szulc A, et al. Relative quantitative PCR to assess bacterial community dynamics during biodegradation of diesel and biodiesel fuels under various aeration conditions. Bioresour Technol. 2011;102:4347–4352.

[34] Grant CE, May DL, Deeley RG. DNA binding and transcription activation by chicken interferon regulatory factor-3 (chIRF-3). Nucleic Acids Res. 2000;28:4790–4799.

[35] Au WC, Moore PA, LaFleur DW, et al. Characterization of the interferon regulatory factor-7 and its potential role in the transcription activation of interferon A genes. J Biol Chem. 1998;273:29210–29217.

[36] Honda K, Yanai H, Negishi H, et al. IRF-7 is the master regulator of type-I interferon-dependent immune responses. Nature. 2005;434:772–777.

[37] Ikushima H, Negishi H, Taniguchi T. The IRF family transcription factors at the interface of innate and adaptive immune responses. Cold Spring Harb Symp Quant Biol. 2013;78:105–116.

[38] Randall RE, Goodbourn S. Interferons and viruses: an interplay between induction, signalling, antiviral responses and virus countermeasures. J Gen Virol. 2008;89:1–47.

[39] Huang B, Qi ZT, Xu Z, et al. Global characterization of interferon regulatory factor (IRF) genes in vertebrates: glimpse of the diversification in evolution. BMC Immunol. 2010;11:22.

[40] Lee CH, Melchers M, Wang H, et al. Regulation of the germinal center gene program by interferon (IFN) regulatory factor 8/IFN consensus sequence-binding protein. J Exp Med. 2006;203:63–72.

[41] Tsujimura H, Tamura T, Ozato K. Cutting edge: IFN consensus sequence binding protein/IFN regulatory factor 8 drives the development of type I IFN-producing plasmacytoid dendritic cells. J Immunol. 2003;170:1131–1135.

[42] Tailor P, Tamura T, Kong HJ, et al. The feedback phase of type I interferon induction in dendritic cells requires interferon regulatory factor 8. Immunity. 2007;27:228–239.

[43] Negishi H, Taniguchi T, Yanai H. The Interferon (IFN) class of cytokines and the IFN regulatory factor (IRF) transcription factor family. Cold Spring Harb Perspect Biol. 2018;10.

[44] Khatri M, Sharma JM. Infectious bursal disease virus infection induces macrophage activation via p38 MAPK and NF-kappaB pathways. Virus Res. 2006;118:70–77.

[45] Palmquist JM, Khatri M, Cha RM, et al. In vivo activation of chicken macrophages by infectious bursal disease virus. Viral Immunol. 2006;19:305–315.

[46] Ovstebo R, Olstad OK, Brusletto B, et al. Identification of genes particularly sensitive to lipopolysaccharide (LPS) in human monocytes induced by wild-type versus LPS-deficient Neisseria meningitidis strains. Infect Immun. 2008;76:2685–2695.

[47] Zhang B, Liu X, Chen W, et al. IFIT5 potentiates anti-viral response through enhancing innate immune signaling pathways. Acta Biochim Biophys Sin (Shanghai). 2013;45:867–874.

[48] Zhou Z, OJ H, Ank N, et al. Type III interferon (IFN) induces a type I IFN-like response in a restricted subset of cells through signaling pathways involving both the Jak-STAT pathway and the mitogen-activated protein kinases. J Virol. 2007;81:7749–7758.

[49] Stirnweiss A, Ksienzyk A, Klages K, et al. IFN regulatory factor-1 bypasses IFN-mediated antiviral effects through viperin gene induction. J Immunol. 2010;184:5179–5185.

[50] Szretter KJ, Brien JD, Thackray LB, et al. The interferon-inducible gene viperin restricts West Nile virus pathogenesis. J Virol. 2011;85:11557–11566.

[51] Gack MU, Shin YC, Joo CH, et al. TRIM25 RING-finger E3 ubiquitin ligase is essential for RIG-I-mediated antiviral activity. Nature. 2007;446:916–920.

[52] Shao Q, Xu W, Yan L, et al. Function of duck RIG-I in induction of antiviral response against IBDV and avian influenza virus on chicken cells. Virus Res. 2014;191:184–191.

[53] Stark GR, Darnell JE. The JAK-STAT Pathway at Twenty. Immunity. 2012;36::503–514.

[54] Schoggins JW, Wilson SJ, Panis M, et al. A diverse range of gene products are effectors of the type I interferon antiviral response. Nature. 2011;472:481–485.

[55] Schoggins JW, MacDuff DA, Imanaka N, et al. Pan-viral specificity of IFN-induced genes reveals new roles for cGAS in innate immunity. Nature. 2014;505:691–695.